The Crystal Structure of the R52Q Mutant Demonstrates a Role for R52 in Chromophore pK_a Regulation in Photoactive Yellow Protein[†,‡]

Nobutaka Shimizu,[§] Hironari Kamikubo,[||] Yoichi Yamazaki,[||] Yasushi Imamoto,[||] and Mikio Kataoka*[,||]

Graduate School of Materials Science, Nara Institute of Science and Technology, Ikoma, Nara 630-0192, Japan, and Structural Biology Group, Research and Utilization Division, Japan Synchrotron Radiation Research Institute, Hyogo, Japan

Received July 21, 2005; Revised Manuscript Received January 19, 2006

ABSTRACT: Mutating arginine 52 to glutamine (R52Q) in photoactive yellow protein (PYP) increases the pK_a of the chromophore by 1 pH unit. The structure of the R52Q PYP mutant was determined by X-ray crystallography and was compared to the structure of wild-type PYP to assess the role of R52 in pK_a regulation. The essential differences between R52Q and the wild type were confined to the loop region containing the 52nd residue. While the hydrogen bonds involving the chromophore were unchanged by the mutation, removing the guanidino group generated a cavity near the chromophore; this cavity is occupied by two water molecules. In the wild type, R52 forms hydrogen bonds with T50 and Y98; these hydrogen bonds are lost in R52Q. Q52 is linked to Y98 by hydrogen bonding through the two water molecules. R52 acts as a lid on the chromophore binding pocket and controls the accessibility of the exterior solvent and the pK_a of the chromophore. R52 is found to flip out during the formation of PYP_M. The result of this movement is quite similar to the altered structure of R52Q. Thus, we propose that conformational changes at R52 are partly responsible for pK_a regulation during the photocycle.

Photoactive yellow protein (PYP), isolated from the purple sulfur photosynthetic bacterium (*1*) *Halorhodospira halophila,* is thought to be involved in negative phototaxis of the bacterium (*2*). Because PYP is a water-soluble photoreceptor protein, its structure is strikingly different from the structures of other well-known membrane-embedded photoreceptor proteins, such as bacteriorhodopsin and sensory rhodopsins, which utilize retinal as a chromophore. Crystallography (*3*, *4*) and NMR (*5*) have demonstrated that PYP has an α/β-fold structure composed of 125 amino acid residues and *p*-coumaric acid as a chromophore for visible light absorption (*6*−*8*).

The chromophore of PYP is buried inside the protein and is bound to Cys69 by a thioester bond. In the dark state, the *p*-coumaric acid chromophore is deprotonated. The pK_a of the chromophore is kept at ∼3, which is much lower than the pK_a of free coumaric acid, ∼9 (*9*). The crystal structure of PYP shows that the chromophore is surrounded by several hydrophilic residues, including Y42, E46, and R52. The phenolic oxygen of the chromophore is hydrogen bonded to Y42 and E46, and this hydrogen bond network is related to the lower pK_a value and the absorption spectrum. In fact, the isosteric mutants, Y42F and E46Q, have altered absorption maxima and pK_a values (*21*, *30*). On the other hand, the positively charged R52 residue does not interact with the chromophore directly, because the R52Q mutant and wild type have identical spectra. However, the pK_a value of R52Q is 1 pH unit higher than that of the wild type (*21*, *30*). This suggests that R52 is involved in pK_a regulation.

PYP has a photoreaction cycle comprised of several intermediate states (*10*−*13*). In the initial step of this cycle, the chromophore is photoisomerized to the cis form (*14*). The phenolic oxygen is then protonated (*15*, *16*). This protonation is regulated by changes in the pK_a of the chromophore during the photocycle. Therefore, elucidating the mechanism of chromophore pK_a regulation will help us understand the mechanism of PYP activation by light. As the PYP protein converts to the PYP_M[1] (also called I_2 and pB) intermediate, a global conformational change occurs (*17*−*19*). Because PYP_M is the longest-lived (130 ms) of the intermediates and is the sole intermediate with an absorption maximum in the ultraviolet region ($\lambda_{max} \sim 360$ nm), it is presumed to be the physiologically active state. We have suggested that R52 is involved in target recognition (*20*). The crystal structure of pB (PYP_M) was determined by time-resolved Laue X-ray diffraction (*18*). The determined crystal structure demonstrated that the side chain of R52 is exposed to the solvent, resulting in the appearance of a cavity near the loop containing R52.

The structure of the R52Q mutant was determined by X-ray crystallography and compared to the structure of the wild type to elucidate the role of R52 in pK_a regulation. The essential differences between R52Q and the wild type are

[†] This work was supported in part by a Grant-in-Aid for Scientific Research from the Ministry of Education, Culture, Sports, Science and Technology of Japan.

[‡] The coordinates have been deposited as Protein Data Bank entries 2D01 for the wild type and 2D02 for R52Q.

* To whom correspondence should be addressed. Phone: +81-743-72-6100. Fax: +81-743-72-6109. E-mail: kataoka@ms.naist.jp.

[§] Japan Synchrotron Radiation Research Institute.

[||] Nara Institute of Science and Technology.

[1] Abbreviations: PYP_L, L intermediate of PYP; PYP_M, M intermediate of PYP; λ_{max}, absorption maximum in the visible region; rmsd, root-mean-square deviation; R_g, radius of gyration.

10.1021/bi051430a CCC: $33.50
Published on Web 02/22/2006

localized at the loop containing the 52nd residue. The removal of the guanidino group disrupts the hydrogen bond between R52 and Y98. The loop containing R52 moves away from the opposite loop, generating a cavity in the interior of the protein. Further, the outward movement of the loop promotes the penetration of two water molecules into the cavity; we propose that this increases the pK_a of the chromophore. The structural changes in the wild-type protein that occur during the photocycle seem to be mimicked by the changes caused by mutating R52 to Q. Therefore, cavity generation and the subsequent penetration of water molecules may occur during photoreaction.

MATERIALS AND METHODS

Sample Preparation. Wild-type PYP and R52Q were overexpressed using the pET system in *Escherichia coli* BL21(DE3) (Novagen) and were reconstituted with *p*-coumaric acid anhydride in 4 M urea buffer (*21*). After the urea had been removed by dialysis, the proteins were purified by DEAE-Sepharose CL6B (Amersham Biosciences, Piscataway, NJ) column chromatography several times until the optical purity index (absorbance$_{277}$/absorbance$_{\lambda_{max}}$) was less than 0.44.

Crystallization, Data Collection, and Processing. Crystallization was performed by vapor diffusion at 20 °C. The purified samples were dialyzed against 50 mM sodium citrate buffer at pH 6.0 and concentrated to 25 mg/mL using an ultrafiltration membrane (Centricon YM10, Millipore, Bedford, MA). The sample solutions were mixed with a reservoir solution containing 40% polyethylene glycol 2000 and 100 mM sodium citrate at pH 6.5 for the wild type and pH 6.0 for R52Q. Within 2 days, crystals with a fine hexagonal form grew to a suitable size (50 μm × 50 μm × 300 μm) for diffraction measurements. The sample crystals were cryoprotected by being soaked in a reservoir solution containing 5% sucrose, mounted in a fiber loop, and kept at 100 K under a continuous stream of nitrogen gas (Rigaku). X-ray diffraction measurements were performed using synchrotron radiation from BL40B2 at the SPring-8 facility (*22*). Data were recorded on a Quantum 4R CCD detector (ADSC) over a rotation of 180° with an oscillation step of 1.0°. The X-ray wavelength was 1 Å, and the distances from the sample to the detector were 78 mm for the wild type and 100 mm for R52Q. Data were processed and scaled using *HKL2000* (*23*). The results of the data collection are listed in Table 1. Although the crystals of both proteins belonged to the same space group, $P6_5$, the lattice constants were different (Table 1).

Structure Determination and Refinement. Molecular replacement was carried out using AMoRe (*24*). The search model for the molecular replacement was constructed by removing the *p*-coumaric acid chromophore and all of the water molecules from the structure of a $P6_3$ PYP crystal (PDB entry 2PHY) (*3*). For R52Q, residues 42−59 in the model were also omitted. The single solutions with the highest *R*-factor and correlation coefficient were obtained from 7.0 to 4.0 Å data for both structures. Structure refinement and model building were performed with CNS (*25*), Refmac5 (*26*), and O (*27*). The resolution range for the refinement process was 20.0−1.34 Å for the wild type and 20.0−1.42 Å for R52Q. After a few cycles, the *p*-coumaric acid chromophore was placed into the models in $2F_o - F_c$ maps, and some water molecules, which have 4σ peaks in $F_o - F_c$ maps, were added using the water-pick feature of CNS. Residues 42−59 of R52Q, which were clearly seen in the $2F_o - F_c$ maps, were constructed. At the next stage, additional water molecules, which have 3σ peaks in $F_o - F_c$ maps, were added. Side chains with double conformations could be seen at some residues, and the alternate conformation was built and modified. The *R*-factor and R_{free} were 0.198 and 0.224 for the wild type (20.0−1.34 Å) and 0.180 and 0.214 for R52Q (20.0−1.42 Å), respectively. Refmac5 was executed at the final phase of refinement with anisotropic *B* factors. The final models of PYP and R52Q were obtained through an additional few cycles. The final *R*-factor and R_{free} were 0.152 and 0.189 for the wild type (20.0−1.34 Å) and 0.141 and 0.163 for R52Q (20.0−1.42 Å), respectively. Since the main chain of M1 in the wild-type structure was disordered, this residue was omitted in the model. The final structures were evaluated with PROCHECK (*28*). There were no dihedral angles of residues in the disallowed regions of the Ramachandran plot. The structural coordinates have been deposited in the Protein Data Bank as the following entries: 2D01 for the wild type and 2D02 for R52Q. The structural models shown in Figures 1 and 3 were drawn using CueMol (http://www.cuemol.org).

Table 1: Details of the Data Collection and Model Refinement

	wild type	R52Q
space group	$P6_5$	$P6_5$
lattice constants (Å)	$a = b = 40.42$	$a = b = 37.02$
	$c = 118.13$	$c = 129.62$
resolution (Å)	20.09−1.34	25.74−1.42
no. of observed reflections	261423	207122
no. of unique reflections	24448	18946
R_{merge}[a,b]	0.053 (0.302)	0.070 (0.273)
completeness (%)[a]	99.8 (99.8)	99.9 (100.0)
$\langle I/\sigma(I)\rangle$[a]	14.2 (9.09)	17.0 (14.7)
redundancy[a]	11.1 (11.0)	11.1 (11.0)
mosaicity	0.183	0.440
refinement		
resolution (Å)	20.0−1.34	20.0−1.42
R-factor	0.152	0.141
R_{free}	0.189	0.163
rmsd from ideal geometry		
bonds (Å)	0.012	0.013
angles (deg.)	1.49	1.49
no. of atoms	1246	1217
no. of waters	210	207
average *B* factor (Å^2)	16.99	13.25

[a] Values in parentheses are for the highest-resolution shell. [b] $R_{merge} = \sum_{hkl}\sum_i|I_i(hkl) - \langle I(hkl)\rangle|/\sum_{hkl}\sum_i I_i(hkl)$.

RESULTS AND DISCUSSION

The crystal structures of wild-type PYP and the R52Q mutant were determined at 1.34 and 1.42 Å resolution, respectively. The C_α traces of the wild-type and R52Q proteins are shown in Figure 1. The overall tertiary folds of the two proteins are essentially identical (Figure 1). The geometry of the hydrogen bond network involving the chromophore is not significantly affected by the site-directed R52Q substitution. In R52Q, the distances from O4′ of the chromophore to O_η of Y42 and to $O_{\epsilon 2}$ of E46 are 2.5 and 2.6 Å, respectively, which are identical to those observed in the wild-type structure (Figure 3a,b). These values are unusually short, compared with the length of a normal

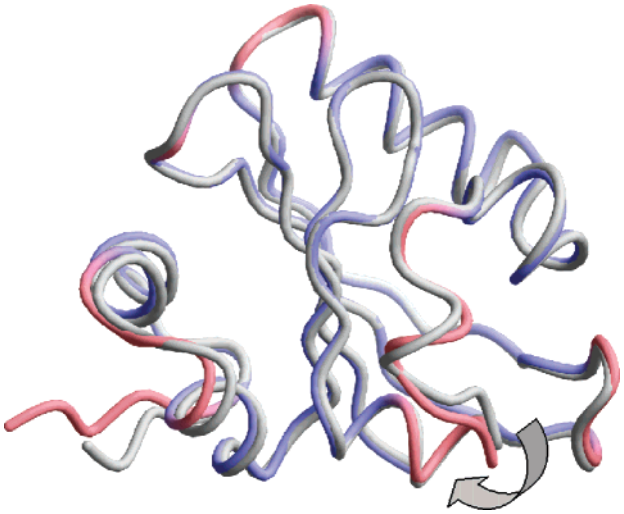

FIGURE 1: C_α traces of the crystal structures of the wild type (gray) and the R52Q mutant. In R52Q, C_α atoms with high rmsd values (>0.5 Å) are colored magenta and other regions cyan. An arrow indicates the movement of the loop including the 52nd residue when R52 is replaced with Q.

hydrogen bond (2.7−3.0 Å). It has been pointed out that the unusually short hydrogen bonds are key elements in controlling the photoreaction (*31*). For precise comparison, the rmsd of R52Q relative to the wild type was examined (Figure 2). The structural differences between the wild-type and R52Q proteins are localized in the N-terminal region (residues 1−5 and 17−21) and the loop including the 52nd residue (residues 47−59). The N-terminal region of R52Q is oriented in a direction different from that of the wild type. The deviation of the C_α of H3 of R52Q relative to that of the wild type is ∼3.0 Å, even though the N-terminal region is far from the position of the mutation. To clarify the basis of this structural deviation, the molecular packing of the R52Q crystal was carefully compared with that of the wild-type crystal. It is interesting that, while both crystals belong to the same space group, $P6_5$, the orientation of the R52Q molecule in the crystal is quite different from that of the wild type. This leads to different molecular packing, especially around the N-terminal region. While the N-terminal region of the wild-type protein closely contacts the adjacent molecule, there is a small cavity between the N-terminal region of R52Q and the adjacent molecule (not shown). Because of the cavity, the lattice constant along the *c*-axis of R52Q is 11.5 Å larger than that of the wild type (Table 1). The N-terminal region in the NMR structural model is widely spread and cannot be determined to be a unique conformation (*5*), suggesting that the N-terminal region of PYP is flexible and easily affected by the environment. The R_g values for the crystal structures of the wild type and R52Q were calculated using CRYSOL (*29*). The difference in R_g values was 0.1 Å, while the experimental values of R_g obtained by small-angle X-ray solution scattering were identical (15.2 Å, data not shown) (*20*). Therefore, the structural difference in the N-terminal regions between the wild-type and R52Q crystal structures is not essential, but merely due to the difference in molecular packing.

Large rmsd values were observed in the region of residues 47−59 of R52Q relative to the wild type; this area is moved away from the opposite loop (residues 98−101) in the mutant structure (arrow in Figure 1). In both the wild-type and R52Q proteins, the region containing residues 47−59 contacts the adjacent molecular surface in the crystal at a similar distance (not shown). Therefore, it is likely that the displacement is due to intrinsic effects of the mutation. Figure 3 compares the structures of the wild type and R52Q near the chromophore. In the wild type (Figure 3a), the guanidino groups ($N_{\eta1}$ and $N_{\eta2}$) of R52 form hydrogen bonds with the amide oxygens (O) of T50 and Y98 at distances of 2.9 and 2.8 Å, respectively. This suggests that the region containing residues 47−59 is connected to the opposite loop (residues 98−101) by hydrogen bonds. In contrast, in the R52Q mutant, these hydrogen bonds are perturbed by the smaller side chain of the Gln residue. The replacement creates a cavity at the position of the guanidino groups in the wild type (Figure 3b). This cavity breaks the direct hydrogen bond observed in wild type, and the distances from $O_{\epsilon1}$ of Q52 to O of T50 and to O of Y98 are extended to 3.9 and 6.8 Å, respectively. It should be noted that the cavity in R52Q is filled with two water molecules (wat27 and wat38) (Figure 3b). The first water molecule (wat27) is 3.1 Å from $O_{\epsilon1}$ of Q52 and 2.9 Å from O of V66, and the second water molecule (wat38) is 2.8 Å from wat27 and 2.9 Å from O of Y98. Therefore, the direct hydrogen bond between R52 and Y98 in the wild type is replaced by a hydrogen bond network among the two water molecules, $O_{\epsilon1}$ of Q52, and O of Y98 in R52Q. The structural deviation observed in R52Q, where the loop moves away from the opposite loop and opens the chromophore binding pocket (Figure 1), is caused by the disruption of the direct hydrogen bond between the two loops, resulting in the penetration of water molecules into the space.

The crystal structure of R52Q can explain the spectroscopic properties of R52Q reported to date (*21*, *30*). The absorption spectrum of R52Q is almost identical with that of the wild type. Therefore, R52 is not responsible for the spectral tuning of PYP. The lengths of hydrogen bonds between O4′ of the chromophore and Oη of Y42 and between O4′ and Oϵ of E46 are kept constant upon mutation. Further, these data also suggest that the positive charge of R52 does not affect the chromophore electrostatically, because R52Q, which lacks the positive charge but has an identical hydrogen bond network around the chromophore, exhibits the same spectrum as the wild type (*21*, *30*).

On the other hand, a pH titration study showed that the pK_a of the chromophore of R52Q exhibits an increase of 1.0 pH unit relative to that of the wild type (*21*, *30*). Because R52 does not interact with the chromophore electrostatically, the increased pK_a is not due to the replacement of the positively charged amino acid residue with the neutral one. As shown above, the inherent structural difference between R52Q and the wild type is confined to the region around the 52nd residue. The removal of the guanidino group generates a cavity, which is occupied by two water molecules. The hydrogen bonds of R52 to T50 and Y98 in the wild type are substituted with a hydrogen bond network extending from Q52 to Y98 through these two water molecules (Figure 3). Therefore, R52 prevents water molecules from penetrating the chromophore binding pocket in the wild-type protein; thus, the phenolic oxygen of the chromophore is spatially separated from the nearest water molecule by 7.6 Å (wat105 in Figure 3a). In contrast, in R52Q, two water molecules are located at the position of

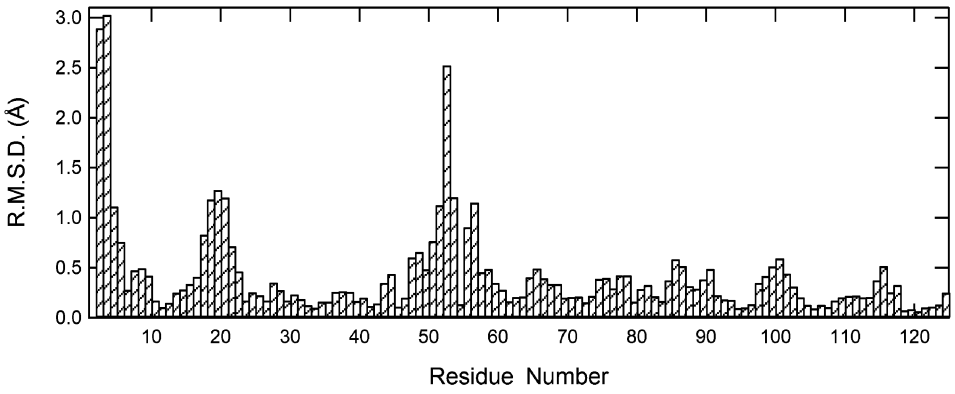

FIGURE 2: C_α rmsd values of R52Q relative to the wild type.

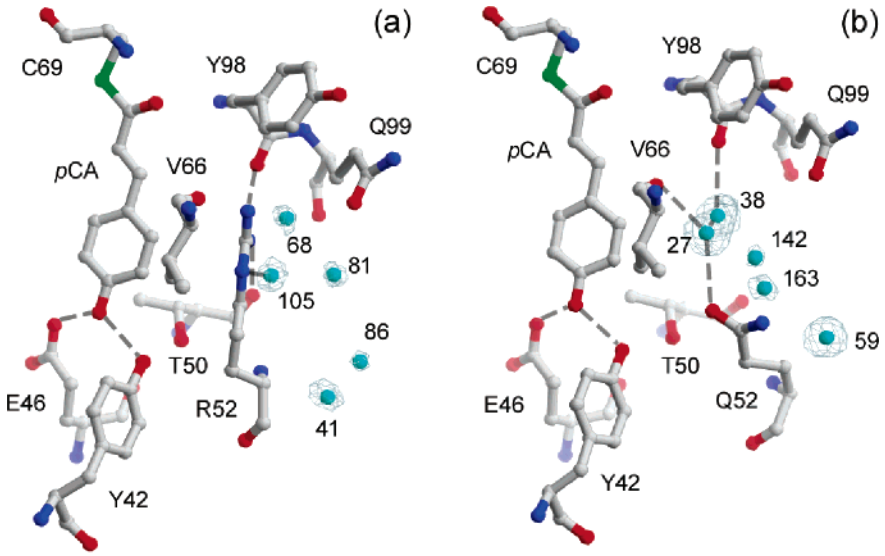

FIGURE 3: Structures of the wild type (a) and R52Q (b) in the vicinity of the chromophore. Carbon atoms are colored gray, oxygens red, nitrogens blue, and sulfurs green. $F_o - F_c$ maps contoured at 4σ are superimposed on water molecules. The hydrogen bonds are represented by dashed lines.

the eliminated guanidine group, and the distance between one of the water molecules (wat27) and the chromophore is 6.0 Å. These results suggest that both the loss of the original hydrogen bonds of R52 and the presence of the two occupying water molecules contribute to the increased pK_a of the chromophore in R52Q.

A recent SVD analysis of time-resolved difference electron density maps showed that the hydrogen bonds of R52 are maintained in the pR (PYP_L) intermediate and that the R52 residue moves away from the opposite loop during formation of the pB (PYP_M) intermediate, disrupting the hydrogen bonds (*19*). No information about water molecules was obtained from the structural model of PYP_M in that study due to insufficient data statistics (*19*). However, this study of the structure of the R52Q mutant has shown a disruption of the hydrogen bond network at the 52nd residue, which closely mimics the structure around R52 in the wild-type PYP_M intermediate. Therefore, we propose that the flipping motion of R52 is involved in the regulation of the pK_a of the chromophore during PYP_M formation. In this model, a conformational change and the subsequent penetration of water molecules into the chromophore binding pocket modulate the milieu of the chromophore.

In the dark state, the anionic phenolic oxygen of the chromophore is stabilized by a hydrogen bond network involving the phenol oxygen of Y42 and the carboxyl proton of E46. Previous studies of the E46Q and Y42F mutants, both of which have weakened hydrogen bonds to O4′ of the chromophore in the dark state, determined that the pK_a values of the chromophore increased by 2.3 and 1.5 pH units, respectively. Crystallographic studies of these mutants showed that the structural alterations caused by the mutations are localized in the hydrogen bond network (*31*). These observations suggest that the pK_a of the chromophore is closely related to the geometry of the hydrogen bond network, that is, the strength of the hydrogen bonds around the chromophore.

It should be noted that the replacement of R52 with Q results in a 1 pH unit increase in the chromophore pK_a; this is comparable to the effects of E46Q and Y42F. Nevertheless, in this mutant, the hydrogen bonds involving the phenolic oxygen of the chromophore are virtually unchanged within the 1.42 Å resolution, while in the isosteric E46Q and Y42F mutants, the lengths of the hydrogen bonds are altered. The apparent pK_a of the chromophore buried in the interior of the protein is determined by both the stability of the anionic form of the chromophore and the accessibility of the protein interior to the exterior solvent. We propose that the 52nd residue acts as a lid on the chromophore binding pocket and controls the penetration of water molecules that can influence

the pK_a of the chromophore. On the basis of the structural similarity of the loop containing the 52nd residue in the R52Q mutant and the wild-type PYP_M intermediate, we propose that the flipping motion of R52 modulates solvent accessibility and is responsible for the pK_a change during PYP_M formation. If the effects of E46 and Y42 on the pK_a are additive, these two residues contribute an increase of 3.8 pH units. Since the pK_a of the chromophore in the wild-type protein in the dark state is 3, the resultant pK_a would be 6.8, a value insufficient to result in substantial protonation of the chromophore during the photocycle. However, the additional contribution of R52 raises the pK_a to 7.8, resulting in sufficient protonation of the chromophore. This strongly suggests that R52 plays a substantial role in pK_a regulation.

ACKNOWLEDGMENT

We are grateful to Professor Toshio Hakoshima, Dr. Toshiyuki Shimizu, and Dr. Ryoko Maesaki of the Nara Institute of Science and Technology and Dr. Mamoru Suzuki of the Institute of Protein Research at Osaka University for helpful advice in the crystal structure analysis. The X-ray diffraction experiments were performed under the approval of the JASRI Program Advisory Committee (Proposals J03B40B2-0505N and J04A40B2-0501N).

REFERENCES

1. Meyer, T. E. (1985) Isolation and characterization of soluble cytochromes, ferredoxins and other chromophoric proteins from the halophilic phototrophic bacterium *Ectothiorhodospira halophila*, *Biochim. Biophys. Acta 806*, 175−183.
2. Sprenger, W. W., Hoff, W. D., Armitage, J. P., and Hellingwerf, K. J. (1993) The eubacterium *Ectothiorhodospira halophila* is negatively phototactic, with a wavelength dependence that fits the absorption spectrum of the photoactive yellow protein, *J. Bacteriol. 175*, 3096−3104.
3. Borgstahl, G. E. O., Williams, D. R., and Getzoff, E. D. (1995) 1.4 Å structure of photoactive yellow protein, a cytosolic photoreceptor: Unusual fold, active site, and chromophore, *Biochemistry 34*, 6278−6287.
4. Van Aalten, D., Crielaard, W., Hellingwerf, K. J., and Joshua-Tor, L. (2000) Conformational substrates in different crystal forms of the photoactive yellow protein—correlation with theoretical and experimental flexibility, *Protein Sci. 9*, 64−72.
5. Düx, P., Rubinstenn, G., Vuister, G. W., Boelens, R., Mulder, F. A., Hård, K., Hoff, W. D., Kroon, A. R., Crielaard, W., Hellingwerf, K. J., and Kaptein, R. (1998) Solution structure and backbone dynamics of the photoactive yellow protein, *Biochemistry 37*, 12689−12699.
6. Hoff, W. D., Düx, P., Hård, K., Devreese, B., Nugteren-Roodzant, I. M., Crielaard, W., Boelens, R., Kaptein, R., Van Beeumen, J., and Hellingwerf, K. J. (1994) Thiol ester-linked *p*-coumaric acid as a new photoactive prosthetic group in a protein with rhodopsin-like photochemistry, *Biochemistry 33*, 13959−13962.
7. Baca, M., Borgstahl, G. E. O., Boissinot, M., Burke, P. M., Williams, D. R., Slater, K. A., and Getzoff, E. D. (1994) Complete chemical structure of photoactive yellow protein: Novel thioester-linked 4-hydroxycinnamyl chromophore and photocycle chemistry, *Biochemistry 33*, 14369−14377.
8. Imamoto, Y., Ito, T., Kataoka, M., and Tokunaga, F. (1995) Reconstitution photoactive yellow protein from apoprotein and *p*-coumaric acid derivatives, *FEBS Lett. 374*, 157−160.
9. Kroon, A. R., Hoff, W. D., Fennema, H. P., Gijzen, J., Koomen, G. J., Verhoeven, J. W., Crielaard, W., and Hellingwerf, K. J. (1996) Spectral tuning, fluorescence, and photoactivity in hybrids of photoactive yellow protein, reconstituted with native or modified chromophores, *J. Biol. Chem. 271*, 31949−31956.
10. Hoff, W. D., Van Stokkum, I. H. M., Van Ramesdonk, H. J., Van Brederode, M. E., Brouwer, A. M., Fitch, J. C., Meyer, T. E., Van Grondelle, R., and Hellingwerf, K. J. (1994) Measurement and global analysis of the absorbance changes in the photocycle of the photoactive yellow protein from *Ectothiorhodospira halophila*, *Biophys. J. 67*, 1691−1705.
11. Imamoto, Y., Kataoka, M., and Tokunaga, F. (1996) Photoreaction cycle of photoactive yellow protein from *Ectothiorhodospira halophila* studied by low-temperature spectroscopy, *Biochemistry 35*, 14047−14053.
12. Ujj, L., Devanathan, S., Meyer, T. E., Cusanovich, M. A., Tollin, G., and Atkinson, G. H. (1998) New photocycle intermediates in the photoactive yellow protein from *Ectothiorhodospira halophila*: Picosecond transient absorption spectroscopy, *Biophys. J. 75*, 406−412.
13. Imamoto, Y., Kataoka, M., Tokunaga, F., Asahi, T., and Masuhara, H. (2001) Primary photoreaction of photoactive yellow protein studied by subpicosecond-nanosecond spectroscopy, *Biochemistry 40*, 6047−6052.
14. Imamoto, Y., Shirahige, Y., Tokunaga, F., Kinoshita, T., Yoshihara, K., and Kataoka, M. (2001) Low-temperature Fourier transform infrared spectroscopy of photoactive yellow protein, *Biochemistry 40*, 8997−9004.
15. Xie, A., Hoff, W. D., Kroon, A. R., and Hellingwerf, K. J. (1996) Glu46 donates a proton to the 4-hydroxycinnamate anion chromophore during the photocycle of photoactive yellow protein, *Biochemistry 35*, 14671−14678.
16. Imamoto, Y., Mihara, K., Hisatomi, O., Kataoka, M., Tokunaga, F., Bojkova, N., and Yoshihara, K. (1997) Evidence for proton transfer from Glu-46 to the chromophore during the photocycle of photoactive yellow protein, *J. Biol. Chem. 272*, 12905−12908.
17. Brudler, R., Rammelsberg, R., Woo, T. T., Getzoff, E. D., and Gerwert, K. (2001) Structure of the I1 early intermediate of photoactive yellow protein by FTIR spectroscopy, *Nat. Struct. Biol. 8*, 265−270.
18. Xie, A., Kelemen, L., Hendriks, J., White, B. J., Hellingwerf, K. J., and Hoff, W. D. (2001) Formation of a new buried charge drives a large-amplitude protein quake in photoreceptor activation, *Biochemistry 40*, 1510−1517.
19. Ihee, H., Rajagopal, S., Srajer, V., Pahl, R., Anderson, S., Schmidt, M., Schotte, F., Anfinrud, P. A., Wulff, M., and Moffat, K. (2005) Visualizing reaction pathways in photoactive yellow protein from nanoseconds to seconds, *Proc. Natl. Acad. Sci. U.S.A. 102*, 7145−7150.
20. Shimizu, N., Kamikubo, H., Mihara, K., Imamoto, Y., and Kataoka, M. (2002) Effect of Organic Anions on the Photoreaction of Photoactive Yellow Protein, *J. Biochem. 132*, 257−263.
21. Mihara, K., Hisatomi, O., Imamoto, Y., Kataoka, M., and Tokunaga, F. (1997) Functional expression and site-directed mutagenesis of photoactive yellow protein, *J. Biochem. 121*, 876−880.
22. Miura, K., Kawamoto, M., Inoue, K., Yamamoto, M., Kumasaka, T., Sugiura, M., Yamano, A., and Moriyama, H. (2000) Commissioning for wide-angle routine proteomix beamline BL40B2: Protein crystallography and small angle scattering, *SPring-8 User Experiment Report 4*, 168.
23. Otwinowski, Z., and Minor, W. (1997) Processing of X-ray Diffraction Data Collected in Oscillation Mode, *Methods Enzymol. 276*, 307−326.
24. Navaza, J. (1994) AMoRe: An automated package for molecular replacement, *Acta Crystallogr. A50*, 157−163.
25. Brünger, A. T., Adams, P. D., Clore, G. M., DeLano, W. L., Gros, P., Grosse-Kunstleve, R. W., Jiang, J. S., Kuszewski, J., Nilges, M., Pannu, N. S., Read, R. J., Rice, L. M., Simonson, T., and Warren, G. L. (1998) Crystallography & NMR system: A new software suite for macromolecular structure determination, *Acta Crystallogr. D54*, 905−921.
26. Murshudov, G. N., Vagin, A. A., and Dodson, E. J. (1997) Refinement of Macromolecular Structures by the Maximum-Likelihood Method, *Acta Crystallogr. D53*, 240−255.
27. Jones, T. A., Zou, J. Y., Cowan, S. W., and Kjeldgaard, M. (1991) Improved methods for building protein models in electron density maps and the location of errors in these models, *Acta Crystallogr. A47*, 110−119.
28. Laskowski, R. A., MacArthur, M. W., Moss, D. S., and Thornton, J. M. (1993) PROCHECK: A program to check the stereochemical quality of protein structures, *J. Appl. Crystallogr. 26*, 283−291.
29. Svergun, D., Barberato, C., and Koch, M. H. J. (1995) CRYSOL: A program to evaluate X-ray solution scattering of biological

macromolecules from atomic coordinates, *J. Appl. Crystallogr. 28*, 768−773.
30. Imamoto, Y., Koshimizu, H., Mihara, K., Hisatomi, O., Mizukami, T., Tsujimoto, K., Kataoka, M., and Tokunaga, F. (2001) Roles of amino acid residues near the chromophore of photoactive yellow protein, *Biochemistry 40*, 4679−4685.
31. Anderson, S., Crosson, S., and Moffat, K. (2004) Short hydrogen bonds in photoactive yellow protein, *Acta Crystallogr. D60*, 1008−1016.

BI051430A